BBA - Molecular Basis of Disease 1865 (2019) 1379–1388

Contents lists available at ScienceDirect

BBA - Molecular Basis of Disease

journal homepage: www.elsevier.com/locate/bbadis

FMRpolyG alters mitochondrial transcripts level and respiratory chain complex assembly in Fragile X associated tremor/ataxia syndrome [FXTAS]

Dhruv Gohel[a], Lakshmi Sripada[a], Paresh Prajapati[b], Kritarth Singh[a], Milton Roy[a], Darshan Kotadia[a], Flora Tassone[d], Nicolas Charlet-Berguerand[c], Rajesh Singh[a,*]

[a] Department of Biochemistry, Faculty of Science, The M.S. University of Baroda, Vadodara 390002, Gujarat, India
[b] SCoBIRC Department of Neuroscience, University of Kentucky, 741S. Limestone, BBSRB, Lexington, KY 40536, USA
[c] Institut de Genetique et de Biologie Moleculaire et Cellulaire (IGBMC), INSERM U964, CNRS UMR7104, Université of Strasbourg, 67400 Illkirch, France
[d] Medical Investigation of Neurodevelopmental Disorders (MIND) Institute, University of California Davis, Davis, CA 95817, USA

ARTICLE INFO

Keywords:
FXTAS
RAN translation
FMRpolyG
Mitochondria
Mitochondrial supercomplexes (mSCs)

ABSTRACT

Fragile X-associated tremor/ataxia syndrome (FXTAS) is an inherited neurodegenerative disorder caused by an expansion of 55 to 200 CGG repeats (premutation) in *FMR1*. These CGG repeats are Repeat Associated non-ATG (RAN) translated into a small and pathogenic protein, FMRpolyG. The cellular and molecular mechanisms of FMRpolyG toxicity are unclear. Various mitochondrial dysfunctions have been observed in FXTAS patients and animal models. However, the causes of these mitochondrial alterations are not well understood. In the current study, we investigated interaction of FMRpolyG with mitochondria and its role in modulating mitochondrial functions. Beside nuclear inclusions, FMRpolyG also formed small cytosolic aggregates that interact with mitochondria both in cell and mouse model of FXTAS. Importantly, expression of FMRpolyG reduces ATP levels, mitochondrial transmembrane potential, mitochondrial supercomplexes assemblies and activities and expression of mitochondrial DNA encoded transcripts in cell and animal model of FXTAS, as well as in FXTAS patient brain tissues. Overall, these results suggest that FMRpolyG alters mitochondrial functions, bioenergetics and initiates cell death. The further study in this direction will help to establish the role of mitochondria in FXTAS conditions.

1. Introduction

Fragile X-associated tremor/ataxia syndrome (FXTAS) is a neurodegenerative disorder characterized by progressive intention tremor (parkinsonism), gait ataxia and cognitive decline [1]. In addition, neuropathy, thyroid dysfunctions, hypertension, immune dysfunction and cardiac arrhythmias are also observed in some patients of FXTAS [2]. FXTAS affects 1 in ~3000 male and 1 in ~5000 female and disease symptoms get more pronounced with the age [3]. The Fragile X mental retardation (*FMR1)* gene, located on the q-arm of the chromosome X, encodes for the FMRP-RNA binding protein, which is involved in regulation of transport and local translation of mRNAs in brain and is essential to synaptic plasticity and neuronal development [4–6]. An expansion of CGG trinucleotide repeats within the 5′-UTR of *FMR1* causes different neuropathological conditions based on the number of CGG repeats.

Firstly, expansions exceeding 200 CGG repeats, which are called full mutations, are the main cause of Fragile X syndrome (FXS), a neurodevelopmental disease characterized by intellectual disability and autism. Expansions over 200 CGG repeats lead to hypermethylation and silencing of the *FMR1* promoter. Hence, the FMRP protein encoded by *FMR1* is absent, which ultimately results in alterations of the brain synaptic plasticity [7]. Secondly, Fragile X-associated Tremor/Ataxia Syndrome (FXTAS) is caused by presence of 55 to 200 CGG repeats, which is named premutation [8]. The prevalence of the CGG premutation carrier varies among populations but is estimated to range between 1 in 110 to 250 in females and 1 in 260 to 800 in males [9,10]. At the histopathological level, FXTAS is characterized by neuronal cell loss and presence of large ubiquitin-positive intranuclear inclusions in both neurons and astrocytes [11]. Rare ubiquitin positive inclusions are also observed in non-CNS organs like kidney and thyroid [12]. At the molecular level and in strict contrast to Fragile-X, the CGG premutation expansion does not inhibit but promotes *FMR1* expression in FXTAS, resulting in 2 to 8 folds higher levels of *FMR1* mRNA in FXTAS patients compared to control individuals [13,14]. Importantly, expression of mutant RNA containing the CGG premutation is pathogenic both in cell and animal models [15–20]. Studies in the last decade have identified two main mechanisms of how CGG repeats expression can be toxic for

* Corresponding author.
E-mail address: rajesh.singh-biochem@msubaroda.ac.in (R. Singh).

https://doi.org/10.1016/j.bbadis.2019.02.010
Received 12 July 2018; Received in revised form 6 February 2019; Accepted 11 February 2019
Available online 13 February 2019

neurons: RNA mediated titration of specific RNA binding proteins and Repeat Associated non-ATG (RAN) translation of the CGG premutation into toxic proteins [21–26]. In that aspect, several emerging evidences indicate that translation initiation to near-cognate start codons located before the CGG premutation leads to expression of a small polyglycine-rich protein named FMRpolyG. FMRpolyG is prone to aggregation and forms large nuclear ubiquitin-positive inclusions in both cells and animals. Importantly, FMRpolyG expression appears mandatory to mediate the toxicity of the CGG premutation in cells, *Drosophila* and mouse models of FXTAS [27,28]. However, how FMRpolyG causes neuronal cell dysfunctions and cell death is currently unclear.

Mitochondrial dysfunctions are one of the major hallmarks of neurodegenerative diseases, including FXTAS. Various studies had shown mitochondrial dysfunctions in cell and mouse models of FXTAS as well as in fibroblasts and brain tissue of premutation carriers [29–31]. However, the cellular and molecular mechanisms triggering mitochondrial dysfunctions in FXTAS are not well understood. In the current study, we investigated the FMRpolyG interaction with mitochondria and its role in modulation of mitochondrial functions using different *in vitro* cellular systems and animal model. We found that FMRpolyG, apart from forming nuclear inclusions, also forms small inclusions that interact with mitochondria. Furthermore, FMRpolyG expression recapitulates mitochondrial dysfunctions identified in FXTAS, including decreased levels of ATP and elevated production of ROS. The defects in mitochondrial complexes assembly and decreased expression of mitochondrial DNA encoded transcripts were observed in both FMRpolyG expressing condition We confirmed these results in mouse models of FXTAS and in tissue samples of individuals with FXTAS. Overall, these data suggest that RAN translation of the CGG premutation may cause the mitochondrial dysfunctions observed in FXTAS.

2. Materials and methods

2.1. Cell culture and reagents

HEK293 cells were grown in Dulbecco's Modified Eagle's Medium (DMEM, Gibco, Invitrogen, USA), SH-SY5Y cells were grown in DMEM-F12 (Gibco, Invitrogen, USA), and U87MG cells were grown in MEM (Minimal Essential Medium, Gibco, Invitrogen, USA) at 37 °C, 5% CO2 and supplemented with 10% (v/v) heat-inactivated fetal bovine serum (Gibco, Invitrogen, USA), 1% penicillin, streptomycin and neomycin (PSN) antibiotic mixture (Gibco, Invitrogen, USA).

2.2. Construct details

Mainly three CGG repeats constructs ATG FMRpolyG-GFP, 5'UTR *FMR1* CGG99X (fused with GFP) and 5'UTR *FMR1* CGG99X untagged were used for transfection for mimicking FXTAS condition *in vitro* (Fig. S1 A). mCherry-Mito-7 was a gift from Michael Davidson (Addgene plasmid # 55102).

2.3. FXTAS transgenic mouse model

Double transgenic Nestin-cre + Full 5'UTR *FMR1* mice were described previously [27]. Briefly these mice overexpress 99 CGG repeats embedded in the 5'UTR natural sequence of the human *FMR1*gene. Expression of the premutation is restricted to the nervous system due to the Nestin-cre that removes a LoxP stop polyadenylation cassette located between the CAG promoter and the 5'UTR *FMR1* construct. All mouse procedures were done according protocols approved by the Committee on Animal Resources of the ICS and IGBMC animal facilities and under the French and European authority guidelines.

2.4. Brain tissue samples

Frozen postmortem human cerebellum tissue from four premutation cases, diagnosed with FXTAS, (mean age at death 77.2 yrs., range 67–85 yrs. Mean CGG repeat number = 92.7; range 86–100 CGG repeats), were obtained from the Medical Investigation of Neurodevelopmental Disorders Institute Brain Repository at the University of California at Davis in Sacramento, CA, under approved IRB protocols (University of California, Davis). Frozen postmortem human cerebellum tissue from four age matched controls was obtained frozen from the Brain and Tissue Bank for Developmental Disorders of the National Institute of Child Health and Human Development at the University of Maryland in Baltimore, MD. CGG repeat sizing was determined on genomic DNA isolated by kit-based method (Puregene Kit; Gentra Inc., Minneapolis, MN). A combination of polymerase chain reaction (PCR) and southern blot (SB) analysis was performed as described previously [32,33]. Total RNA was isolated using TRIzol reagent, quantified and cDNA was synthesized using PrimeScript™ 1st strand cDNA Synthesis Kit (Takara). Realtime PCR was performed to assay the levels of all mitochondrial DNA encoded transcripts.

2.5. Cell death assay and Caspase 3/7 activity

HEK293 and SH-SY5Y cells were plated at density of 5×10^4 cells/well in 96 well plate and transfected with indicated constructs. After 24 h of transfection, MTT assay was performed to check cellular viability [34] and LDH release assay was performed to check cytotoxicity as described previously [35]. Caspase 3/7 activity was measured by using Caspase-Glo® 3/7 Assay Systems (Promega) as per the described protocol.

2.6. Immunohistochemistry and confocal microscopy

The subcellular localization of FMRPolyG, and interaction of cytosolic FMRPolyG with mitochondria was analyzed by confocal microscopy. Briefly, HEK293 cells were plated at density of 1.5×10^5 cells per well in glass bottom 24 well plate (Greiner Bio-One, USA). Cells were co-transfected with mCherry-Mito-7 with ATG FMRpolyG-GFP and 5'UTR *FMR1* CGG99X fused with GFP using Lipofectamine® 2000 (Thermofisher, USA). After 24 h of transfection, cells were fixed and intracellular localization and colocalization of FMRpolyG with mitochondria was analyzed using Leica TCS-SP5II confocal microscope (Leica Microsystems, Germany).

Mouse brain sections were deparaffinized for 20 min in Histosol Plus (Shandon) and dehydrated as follows: twice in ethanol 100% (5 min), twice in ethanol 95% (5 min), once in ethanol 80% (5 min), once in ethanol 70% (5 min) and rinsed in DPBS. Glass coverslips containing brain sections treated as described above, fixed in PFA for 10 min and washed three times with PBS. The coverslips or slides were incubated for 10 min in PBS plus 0.5% Triton X-100 and washed three times with PBS and incubated with primary antibody against FMRpolyG (8FM, 1/100), AIF (1/100, Cell Signaling (USA)). Slides or coverslips were washed twice with PBS and incubated with goat anti-rabbit or goat anti-mouse conjugated with Cyanine 3 (1/500 dilution; Fisher) for 60 min; incubated for 2 min in PBS 1X-DAPI (1/10000 dilution) and rinsed twice with PBS 1X before mounting in Pro-Long media (Molecular Probes). Slides were examined using a fluorescence microscope (Leica). Minimum 30 cells were examined in different conditions for cellular morphology, FMRPolyG localization and interaction with mitochondria. Representative image panel was prepared by Adobe Photoshop CS.

2.7. Western blotting and antibodies

To analyze the presence of FMRPolyG in mitochondria, subcellular fractionation was performed followed by western blotting. Briefly, HEK293 cells were plated at density of 2×10^6 in 90 mm dishes and

transfected with indicated constructs using Lipofectamine® 2000 (Thermofisher, USA). After 24 h of transfection, cells were washed with cold PBS and harvested. Mitochondrial fraction and cytosolic fraction were prepared using Qproteome Mitochondria Isolation Kit (37612, QIAGEN) as per the protocol with minor modifications. Mitochondrial fraction and total cell were resuspended in Triton X-100 IP buffer (150 mM NaCl, 50 mM Tris-HCl, 10% Glycerol, 1% Triton X-100, containing complete protease inhibitor cocktail (Roche, Germany)), incubated on ice for 1 h and centrifuged at 13,000 rpm for 10 min at 4 °C. Protein concentration was quantified by Bradford reagent (BioRad). Protein lysates were separated on 12% SDS-PAGE and analyzed by western blotting using specific antibodies. The primary antibodies used were: Rabbit polyclonal against GFP (AE0011, ABclonal), NDUFS2 (Cell Signaling, USA). Secondary antibodies: HRP-conjugated anti-rabbit and anti-mouse antibodies (Open Biosystems, USA) were used in the study.

2.8. ATP assay

The cellular ATP level was measured using ATP determination kit (Molecular Probes/Life Technologies, Canada) by using 1:10 diluted cell lysate in ATP determination master mix (25 mM Tricine buffer, pH 7.8, 5 mM MgSO4, 0.5 mM D-luciferin, 1.25 μg/ml firefly luciferase, 100 μM EDTA and 1 mM DTT). The luminescence intensity was measured using TriStar^2 LB 942 Multimode Microplate Reader, Berthold Technologies, Germany. The protein content was determined by Bradford assay and equal protein was used for different assays.

2.9. Membrane potential

The mitochondrial membrane potential was determined by staining cells with TMRM (5 μM) (Tetramethylrhodamine, Methyl Ester, Perchlorate, Molecular Probes) for 15 min followed by quantification of fluorescence at 510/570–600 by fluorimeter (Hitachi High-Technologies Corp., Japan). The protein content was determined by Bradford assay and normalized for assay.

2.10. BN-PAGE, colloidal Coomassie blue staining and Ingel activity of mitochondrial respiratory chain complexes

The effect of FMRpolyG on mitochondrial supercomplexes (SCs) assembly and complex-I and complex-IV activity was determined by Blue Native PAGE followed by colloidal Coomassie blue staining and in-gel activity [36]. Briefly, HEK293 and SH-SY5Y cells were seeded at the density of 3×10^6 in 10 cm dishes, transfected with pEGFP-C1 (control), ATG FMRpolyG-GFP and 5'UTR *FMR1* CGG99X. After 24 h of transfection, cells were collected. Similarly, from the brain, cortical region of control as well as FXTAS transgenic mice was collected and homogenized. Isolation of mitochondrial fraction was performed using Qproteome Mitochondria Isolation Kit (37612, QIAGEN). Briefly, the cells (7×10^6) were resuspended in 700 μl lysis buffer. The cells were lysed in disruption buffer using 24G needle and centrifuged at 1000 $\times g$ for 10 min at 4 °C and supernatant collected. The mitochondrial fraction was collected by centrifugation at 6000 $\times g$ for 10 min at 4 °C and purified from the interface of disruption buffer and purification buffer. Mitochondrial protein concentration was determined using the Bradford method and 50 μg mitochondrial protein were solubilized in solubilization buffer (50 mM NaCl, 50 mM Imidazole/HCl pH 7.0, 2 mM 6-aminohexanoic acid, 1 mM EDTA, 6.0 g/g digitonin (10%)) and kept on ice for 30 min. After incubation, solubilized mitochondria were centrifuged for 20 min at 20,000 g. 20 μl supernatant was mixed with 3 μl 50% glycerol and 5% Coomassie blue G-250 (8 g/g detergent to dye ratio). The sample was loaded onto 3–12% acrylamide gradient gel for BN-PAGE, at room temperature and in-gel activity for mitochondrial complex I and complex IV was performed as described previosuly (ref). For visualizing SCs and individual mitochondrial respiratory chain subunits, 100 μg mitochondrial protein was processed and separated by BN-PAGE followed by colloidal Coomassie blue (G-250) staining.

2.11. Analysis of relative mtDNA content and mitochondrial transcripts by qPCR

HEK293 and SH-SY5Y cells were plated at the density of 5×10^5 cells/well in 6 well plate and transfected with pEGFP-C1 (control), ATG FMRpolyG-GFP and 5'UTR *FMR1* CGG99X plasmids using by Lipofectamine® 2000. After 24 h of transfection, cells were collected, and genomic DNA was isolated using phenol: chloroform method [37]. Mitochondrial DNA was quantified by qPCR using RNaseP as endogenous control [38]. RNA was isolated using TRIzol reagent, quantified and cDNA was synthesized using PrimeScript™ 1st strand cDNA Synthesis Kit (Takara). Real-time PCR was performed to assay the levels of all mitochondrial DNA encoded transcripts. Primer sequences used for mouse mitochondrial transcripts are given in Table S1 and for human mito transcripts are given in Table S2.

2.12. Statistical analysis

Data are shown as mean ± SEM for the number of observations. Comparisons of two groups were performed using Student's unpaired *t*-test for repeated measurements to determine the levels of significance for each group. One-paired ANOVA test is used to calculate degree of significance wherever there are more than two groups (Dunnet's multiple comparison test). Each experiment has been repeated minimum two times independently and probability values of $p < 0.05$ were considered as statistically significant.

3. Results

3.1. Expression of expanded CGG repeats decreases cellular viability

To understand the cellular and molecular mechanism of CGG repeats induced toxicity, we transfected a plasmid expressing 99XCGG repeats embedded in the natural sequence of the human *FMR1* gene (Fig. S1 A) in neuronal (SH-SY5Y) and non-neuronal (HEK293) cells. The expression of expanded CGG repeats in HEK293 and SH-SY5Y cells reduces cellular metabolism as evidenced by a decreased production of the colored formazan product that originates from the NAD(P)H-dependent reduction of the MTT tetrazolium dye (Fig. S1 C). To assess whether this deleterious effect was due to the RAN translation of the CGG repeats into FMRpolyG, we assess the effect of expressing FMRpolyG-GFP cloned under the dependency of an artificial ATG start codon (Fig. S1 A). Transfection of FMRpolyG-GFP had a similar deleterious effect than the CGG repeats and decreases cell metabolism in SH-SY5Y cells (Fig. 1C). Treatment with H_2O_2 (100 μM) for 4 h was used as positive control for ROS induced cell death [39]. To differentiate between a decrease in cell metabolism or a reduction of cell viability, we measured the release of lactate dehydrogenase (LDH) enzyme in the media, which indicates damage in cell permeability. LDH release assay demonstrated that expression of the CGG premutation impairs cell membranes compared to control transfections in both HEK293 and SH-SY5Y transfected cells (Fig. 1A and B). Similarly, transfection of a plasmid expressing FMRpolyG-GFP is toxic (Fig. 1A and B). Cell viability was further checked by trypan blue exclusion assay. Trypan blue staining further clarifies the decreased viability in both CGG repeats transfected condition in HEK293 and SH-SY5Y cells (Fig. S1 B). The common signaling cascades involved in apoptosis is the activation of a highly specialized family of cysteinyl-aspartate proteases (caspases) which are usually present as inactive zymogen forms [40]. Hence, we analyzed 3/7 activity. The expression of either expanded CGG repeats or of FMRpolyG-GFP increases caspase 3/7 activity suggesting the activation of caspase dependent apoptosis in HEK-293 (Fig. 1C) and in SH-SY5Y (Fig. 1D) cells. The activation of initiator caspases such as caspase 8 and caspase 9 in both CGG repeats

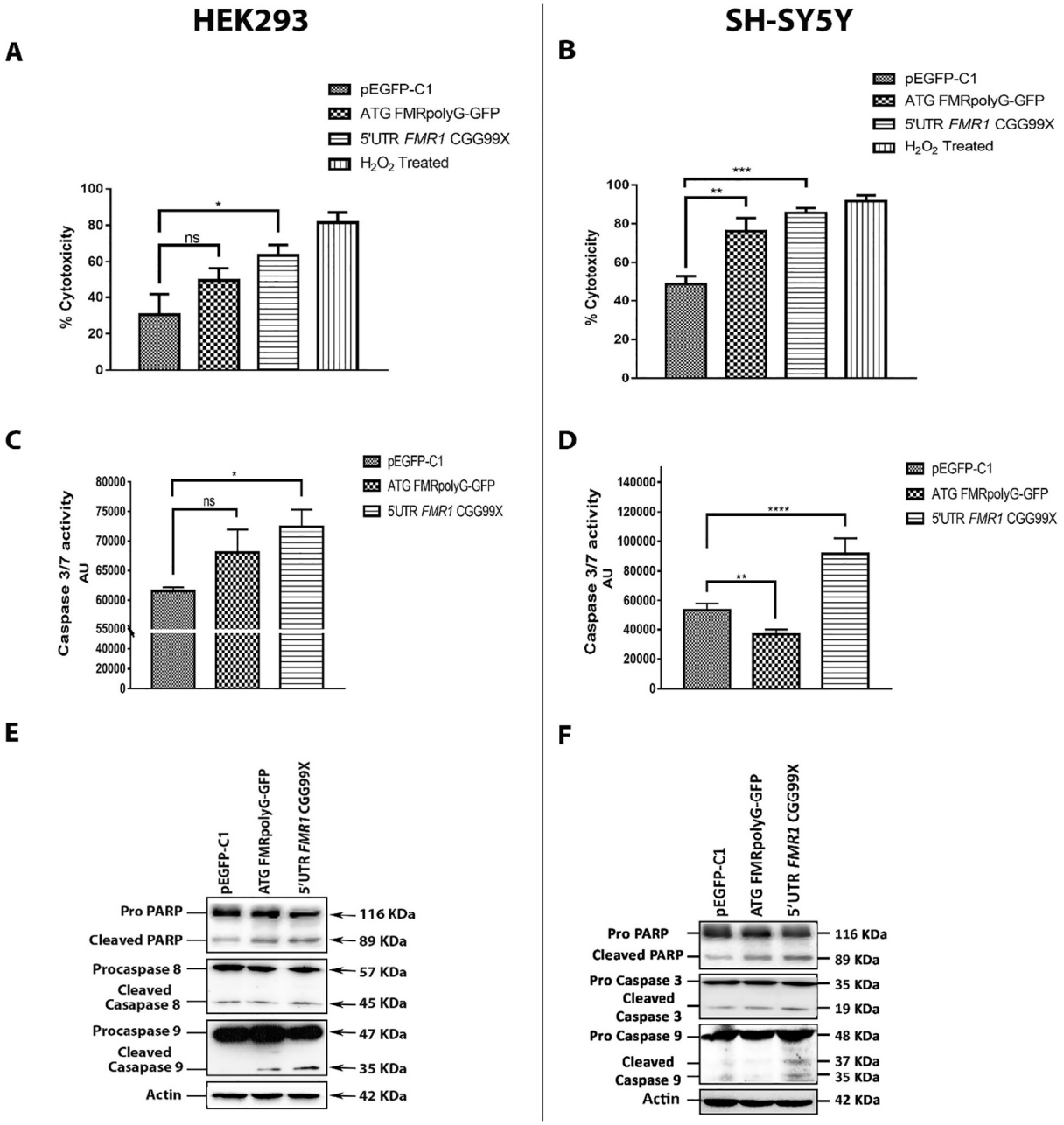

Fig. 1. Expression of expanded CGG repeats increases cellular toxicity and causes apoptotic cell death. Constructs for FMR premutation (ATG FMRpolyG-GFP and 5'UTR *FMR1* CGG99X) along with pEGFP-C1 (control) were transfected and cytotoxicity was measured by LDH release assay in HEK293 (A), and SH-SY5Y (B) cells. Levels of Caspase 3/7 activity was analyzed in HEK293 (C) and SH-SY5Y (D) cells. Western blot analysis was performed for apoptotic markers such as caspase 8, caspase 9, caspase 3 and PARP in HEK293 (E), and SH-SY5Y (F). ($n = 3$) $p > 0.05$ (ns), $p \leq 0.05$ (*), $p \leq 0.01$ (**), $p \leq 0.001$ (***).

transfected condition were analyzed in HEK293 and SH-SY5Y cells. Immunoblotting results showed increased level of 35 KDa band corresponding to the cleaved subunit of caspase 9 under both CGG repeats expressed condition in HEK293 (Fig. 1E) and SH-SY5Y (Fig. 1F) cells. There was no change in cleaved form of caspase 8 in CGG repeats transfected condition as compared to control. These results indicate involvement of mitochondrial mediated apoptosis. Caspase mediated apoptotic cell death is accomplished by the cleavage of several key proteins involving PARP (Poly ADP-ribose polymerase) [41]. Hence, we also checked the levels of pro/cleaved form of PARP. Increased levels of cleaved PARP also suggest the late apoptosis in repeats transfected cells (Fig. 1E, F). Overall, these results confirm that expression of CGG repeats promotes cellular toxicity and induces mitochondrial mediated apoptosis in cells derived from different origin.

3.2. FMRpolyG forms cytosolic inclusions that interacts with mitochondria

Expanded CGG repeats embedded in their natural *FMR1* sequence are RAN translated into the FMRpolyG protein, which form nuclear inclusions [42]. However, their subcellular dynamics of aggregate formation and its interaction with another subcellular organelle before translocation to nucleus is not understood. Hence, we analyzed sub cellular localization of FMRpolyG aggregates. Cell transfection followed by confocal microscopy confirmed that expression of expanded CGG repeats induces formation of large nuclear inclusions of FMRpolyG (Fig. S2). Consistent with a decrease viability upon FMRpolyG expression, cells with nuclear inclusions show altered morphology as they are rounded, vacuolated and show less projections compared to control transfected cells (Fig. S2). Identical results were observed with

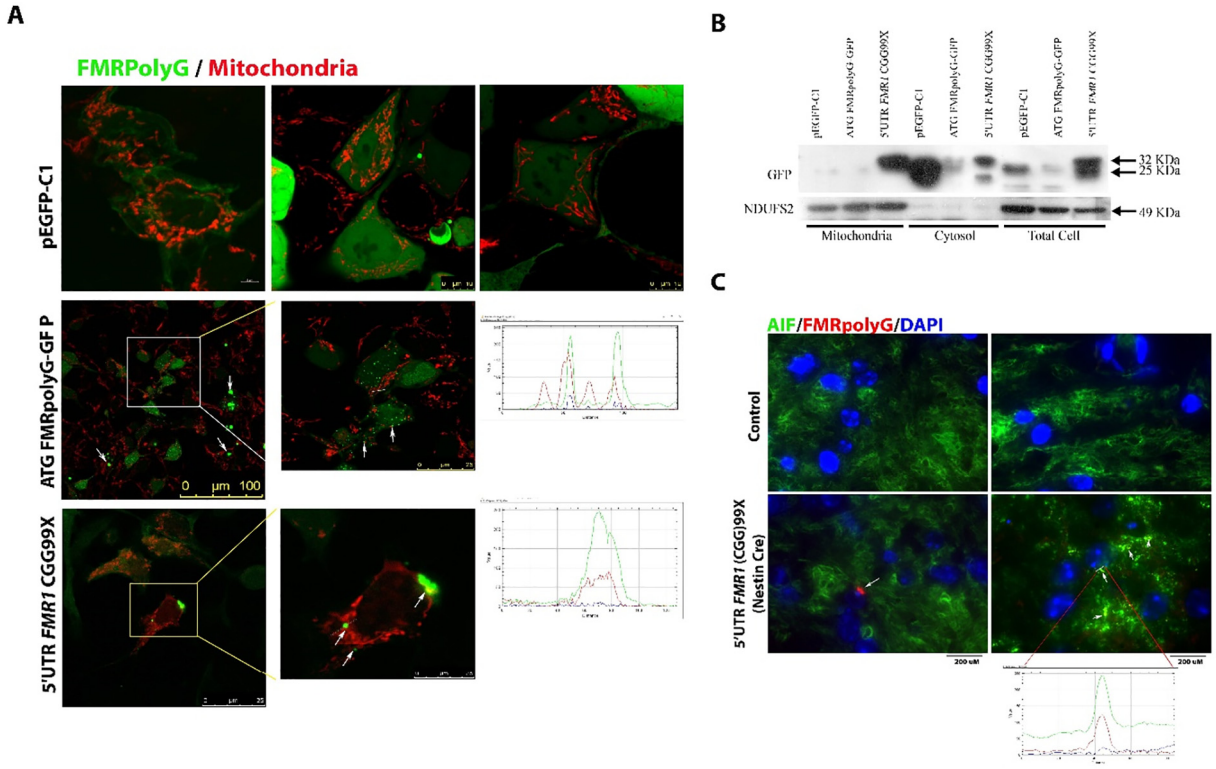

Fig. 2. FMRPolyG forms cytosolic small aggregates and show association with mitochondria. HEK293 cells co-transfected with ATG FMRpolyG-GFP and 5'UTR *FMR1* CGG99X along with mCherry-Mito-7 and observed under confocal microscope for subcellular localization of FMRpolyG. Confocal microscopy showed formation of extra nuclear aggregates visible as green speckles pointed with white arrows. Cytosolic speckles of FMRPolyG are in association with mitochondria (A). Mitochondrial association of FMRpolyG further validated by line intensity plot for overlapping of both (green, red) channels. Immunoblotting against GFP in the different cellular fraction of HEK293 cells transfected with ATG FMRpolyG-GFP and 5'UTR *FMR1* CGG99X. NDUFS2 has been used as mitochondrial marker (B). Translation of FMRpolyG in FXTAS transgenic mice brain tissue section visible as red puncta (8FM) in the nucleus and smaller aggregates showed by white arrows show association with mitochondria (green, AIF) under different resolution. Line intensity profile with both (red/green) channels indicates association of FMRpolyG with mitochondria (C).

transfection of FMRpolyG-GFP expressed under an artificial ATG start codon (Fig. S2). Importantly, we observed that beside formation of large nuclear inclusions, most of CGG repeats or FMRpolyG-GFP transfected cells also show presence of smaller cytosolic aggregates of FMRpolyG (Fig. S3). We further investigated the localization of these small cytosolic FMRpolyG inclusions. Co-transfection of expanded CGG repeats with a mCherry-Mito7 plasmid that labels mitochondria followed by confocal microscopy indicated that the cytosolic FMRpolyG puncta are in contactor on the surface of mitochondria in HEK293 cells (Fig. 2A; S4). Identical results were observed with a plasmid encoding ATG FMRpolyG-GFP (Fig. 2A; S4). To confirm the potential interaction of FMRpolyG with mitochondria, mitochondrial fractions were prepared and analyzed by western blotting. Interestingly, FMRpolyG was observed in the mitochondrial fraction, whereas it was not detected in control GFP transfected cells (Fig. 2B). Finally, presence of small FMRpolyG cytosolic aggregates along with large nuclear inclusions was also observed in FXTAS mouse model. Confocal imaging of FMRpolyG in cortical sections of 2 months old transgenic mice expressing the CGG permutation indicated that the small cytosolic aggregates of FMRpolyG (red) co-localize with AIF (green), a protein marker of mitochondria (Fig. 2C). These observations suggest that FMRpolyG interacts with mitochondria in cell and animal model of FXTAS.

3.3. Expression of FMRpolyG alters mitochondrial functions

As noted previously, expression of the CGG premutation alters mitochondrial functions. We confirmed that expression of CGG repeats decreases cellular ATP levels in both cells (HEK293 and SH-SY5Y) and animal (CGG transgenic mouse) models of FXTAS compared to controls (Fig. 3A). Interestingly, a similar cellular ATP decreased was observed in HEK293 cells upon expression of FMRpolyG-GFP cloned under an artificial ATG (Fig. 3A). Next, we monitored mitochondrial membrane potential using the fluorescent dye TMRM [43]. Similarly decreased mitochondrial membrane potential was observed upon expression of either the CGG premutation or expression of FMRpolyG-GFP (ATG driven) in both non-neuronal HEK-293 and neuronal SH-SY5Y cells (Fig. 3B). The mitochondrial content was also analyzed in the cells expressing FMRpolyG by quantifying mitochondrial/ nuclear DNA ratio by quantitative PCR. The qPCR results indicated that there is no alteration in mitochondrial mass upon expression of FMRpolyG or CGG premutation both in HEK293 and SH-SY5Y cells (Fig. 3C). These results confirm that the CGG premutation alters mitochondrial activities which could be mediated by FMRpolyG interaction with mitochondria.

3.4. CGG permutation alters mitochondrial supercomplexes assembly and affects respiratory chain complex activity

The individual respiratory chain complexes CI, CIII, and CIV associate to form intermediate supramolecular assemblies known as mitochondrial supercomplexes (mSCs), which are required for efficient electron transport and coupling (ETC) [44,45]. The impairment of such supercomplexes formation leads to decline in ETC capasity, cellular respiration and ATP production [46]. BN PAGE followed by colloidal blue staining indicated that expression of the CGG premutation disrupts assemblies of the mitochondrial supercomplexes in both SH-SY5Y (Fig. 4A) and HEK-293 (Fig. 4B) cells. Interestingly, expression of FMRpolyG cloned under an artificial ATG start codon also disrupted respiratory chain super complexes assembly (Fig. 4A and B).

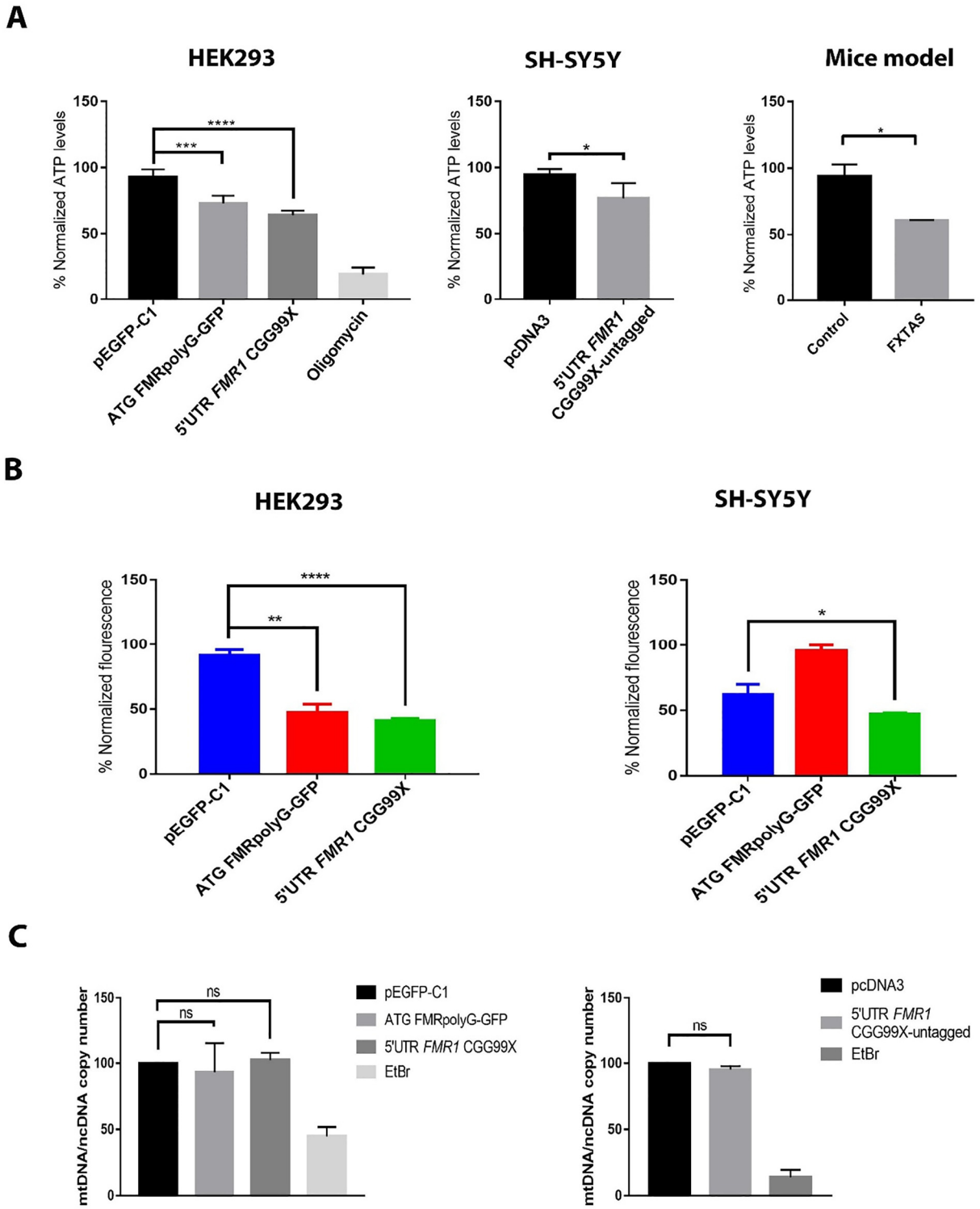

Fig. 3. FMRpolyG alters mitochondrial functions. ATP levels were monitored in ATG FMRpolyG-GFP and 5'UTR *FMR1* CGG99X transfected condition in HEK293, SH-SY5Y cells and in cortical neurons derived from FXTAS transgenic mice ($n = 3$) (A). TMRM staining showing decreased mitochondrial membrane potential in presence of expanded CGG repeats in HEK293 and SH-SY5Y cells (n = 3) (B). mtDNA/ncDNA ratio quantified by qRT-PCR to monitor mitochondrial mass in both the cell lines HEK293 and SH-SY5Y expressing FMRpolyG (C). (n = 3) $p > 0.05$ (ns), $p \leq 0.05$ (*), $p \leq 0.01$ (**), $p \leq 0.001$ (***).

Densitometry analysis was done for intensity quantification of each band in the respective lane (Fig. S5 A). The detailed densitometry analysis in SH-SY5Y and HEK293 suggest decreased levels of SCs labelled as n1-n5 and individual complex II, III, IV in 5'UTR *FMR1* CGG99X compared to control (pEGFP-C1) transfected cells (Fig. S5 B). Mitochondria isolated from cortical region of FXTAS mice model also showed alteration in the levels of supercomplexes intermediate (n1-n5) (Fig. 4C; S5 B). To further determine the specific effect of CGG repeats and FMRpolyG on individual complexes of mitochondrial respiratory chain, we examined the in-gel activity of individual respiratory chain complexes in HEK-293 and in SH-SY5Y cells. Expression of the CGG premutation significantly decreased complex I (NADH dehydrogenase)

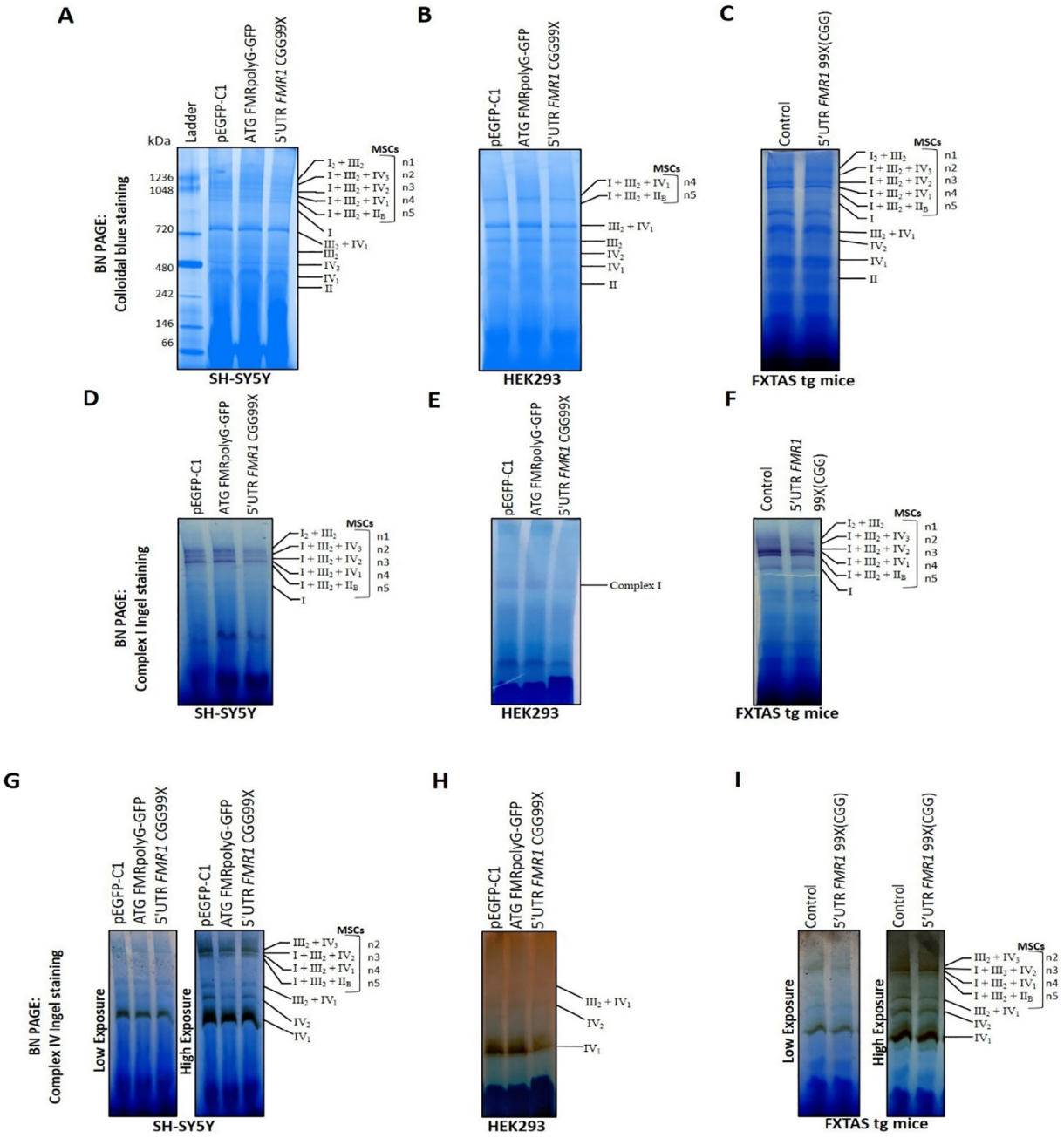

Fig. 4. FMRpolyG formed due to expanded CGG repeats disrupts mitochondrial supercomplexes (SCs) assembly and decreases individual complex activity. SH-SY5Y and HEK293 cells were transfected with ATG FMRpolyG-GFP and 5'UTR *FMR1* CGG99X and mitochondrial supercomplexes (n1-n5) and individual complex levels were detected by gradient BN-PAGE followed by colloidal Coomassie blue staining in SH-SY5Y (A) (n = 3), HEK293 (B) (n = 3) and cortical tissue from FXTAS transgenic mice (C) (*n* = 2). Activity of CI containing supercomplexes and individual CI were determined by BN-PAGE followed by in-gel activity staining specific for CI in SH-SY5Y (n = 3) (D), HEK293 cells (E) (*n* = 4) and in transgenic mice (n = 3) (F). Assembly and activity of CIV containing supercomplexes and individual CIV were determined by gradient BN-PAGE followed by in-gel activity staining specific for CIV in FMRpolyG expressing SH-SY5Y (n = 3) (G), HEK293 (n = 3) (H) and in transgenic mice model (n = 2) with low as well as high time exposure (I).

activity compared to control conditions (Fig. 4D and E). As compare to control, complex I activity is also altered in cortex regions of mice expressing the CGG premutation (Fig. 4F). Densitometry analysis further confirms the decreased complex I activity as shown by decreased area of peak intensities in the graph (Fig. S5 C). Similarly, complex IV (Cytochrome Oxidase) activity is also decreased in cells (Fig. 4G and H) and mice (Fig. 4I) expressing the CGG premutation. These results further confirmed by decreased area of peak intensities under CGG premutation condition in HEK293, SH-SY5Y cells and mice expressing CGG premutation (Fig. S5 D). These observations suggest that the expression of the CGG premutation in cell and animal models induces defects in respiratory chain assembly and individual complex activity.

3.5. FMRpolyG expression alters the level of mitochondrial DNA encoded transcripts

Critical components of the OXPHOS are encoded by the mitochondrial DNA (mtDNA). Thirteen transcripts are encoded by mtDNA: seven transcripts (ND1–ND6 and ND4L) of complex I (NADH: ubiquinone oxidoreductase); one (apocytochrome B) of the complex III (ubiquinol: cytochrome C oxidoreductase) subunits; three (COX1–COX3) of the complex IV (cytochrome *c* oxidase) and two (ATP6 and ATP8) of the

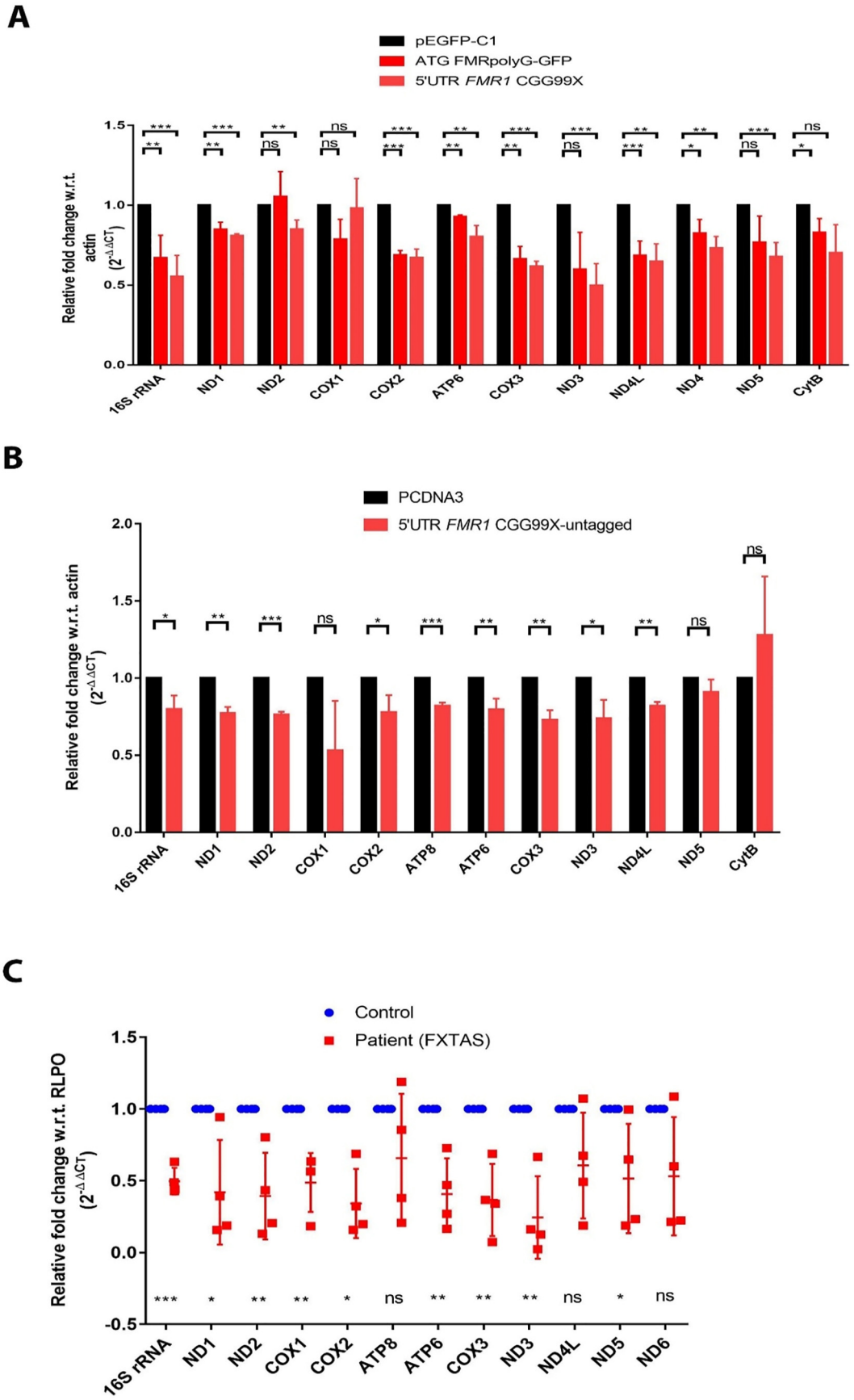

Fig. 5. FMRpolyG alters transcripts encoded by mitochondrial genome. HEK293 and SH-SY5Y cells were transfected with ATG FMRpolyG-GFP and 5'UTR *FMR1* CGG99X. Mitochondrial transcript levels were analyzed by qPCR in HEK293 (A) and SH-SY5Y (B) cells (n = 3). Actin was used as endogenous control. Similarly, mitotranscript levels were checked in FXTAS patients (C), RLPO (large ribosomal protein) was used for endogenous control. (n = 4), $p > 0.05$ (ns), $p \leq 0.05$ (*), $p \leq 0.01$ (**), $p \leq 0.001$ (***).

complex V (ATP synthase)subunits [47]. Hence, critical levels of mitochondrial transcripts should be maintained for optimal mitochondrial functions. To understand how the CGG premutation affects mitochondrial complexes assembly, we analyzed the levels of mitochondrial encoded transcripts. As shown in Fig. 3C, there is no significant change in mitochondrial DNA content in cells expressing the CGG premutation. However, levels of mitochondrial DNA encoded transcripts such as 16S rRNA, ND1, ND3, ND4L, ND4, COX2, COX3 and ATP6 are all reduced in HEK-293 cells expressing the both CGG permutation compared to control (Fig. 5A). Similar results were observed in neuronal SH-SY5Y cells (Fig. 5B). Interestingly, we confirmed these results in brain tissue of FXTAS patients. Quantitative PCR revealed decreased expression of the 16S rRNA, ND1, ND2, ND3, ND5, COX1, COX2, COX3 and ATP6 transcripts in cerebellum samples of individuals with FXTAS compared to control individuals (Fig. 5C). These results suggest that mitochondrial respiratory chain dysfunctions in FXTAS are paralleled by decreased mitochondrial transcripts levels.

4. Discussion

FXTAS is a monogenic disorder caused by an expansion of 55 to 200 CGG repeats located within the 5′-UTR of *FMR1*. Emerging evidences suggest that RAN translation of the CGG permutation into the FMRpolyG protein is an important cause of pathological changes in FXTAS [27,28]. Earlier studies have shown evidence of abnormal mitochondrial function and mitochondrial protein expression in both CNS and non-CNS (dermal fibroblasts) tissues from patients with the FXTAS [12,44,45]. Altered mitochondrial dynamics, mitochondrial dysfunctions and altered metabolic profiles are observed in cell and animal models of FXTAS [29]–[31]. However, how CGG repeats alter mitochondrial functions is not well understood. In the current study, we confirmed that expression of the CGG premutation alters various mitochondrial parameters in cell and animal models which may have implication in FXTAS pathogenesis.

We used neuronal and non-neuronal cells and expressed two constructs mimicking FXTAS conditions to understand the alteration of cellular processes during FXTAS pathogenesis. The enforced expression of FMRpolyG either ATG or RAN translation mimicking native FXTAS condition in different cell lines showed toxicity and inhibited cell proliferation. To further understand the mechanisms regulating neuronal toxicity, we monitored the dynamics of FMRployG aggregates in cells. As reported previously [12] [27] [28], here it was observed that FMRpolyG forms nuclear inclusion. Furthermore, FMRPolyG also forms smaller cytoplasmic aggregates which interact with mitochondria. Importantly, expression of FMRpolyG under an artificial ATG start codon reproduces the deleterious effect of the CGG premutation and leads to multiple alterations of mitochondrial activities. Of technical interest, we used a CGG construct that form little CGG RNA foci but encodes FMRpolyG expressed under an artificial ATG codon [27]. The experiments further suggest that FMRpolyG expression alters mitochondrial functions. The decrease in mitochondrial transmembrane potential and bioenergetic capacity was also observed in FXTAS cells expressing FMRpolyG. This is in consonance with previous observation where mitochondrial functions were altered in fibroblast derived from the FXTAS patients [30,48,49]. Moreover, FMRpolyG also altered mitochondrial architecture in our study, which further suggests that mitochondrial functions may be altered which had been previously reported from FXTAS patients [29]. However, our results are largely based on overexpression systems and do not exclude a potential pathogenic contribution of the CGG repeats at the RNA level. Thus, it remains to test whether endogenous expression of FMRpolyG alters mitochondrial activities. Similarly, analysis of mitochondrial activities upon expression of constructs expressing only CGG repeats *versus* constructs expressing FMRpolyG with optimized codon to exclude CGG repeats toxicity will be necessary to conclude about the relative importance of CGG RNA toxicity *versus* CGG-RAN translation pathogenicity.

How FMRpolyG may alter mitochondrial functions is not clear. Our data indicate that the levels of mitochondrial DNA encoded transcripts decrease in FMRpolyG expressing cells as well as in brain samples of individuals with FXTAS. This is consistent with the observation that all mitochondrial respiratory chain complexes are affected in FXTAS cell and mouse models in this study. Proteomics analysis (Supplementary Table 3) performed in an earlier study [27] showed that several proteins important for mitochondrial activities potentially interact with FMRpolyG. Notably, several of these candidates are involved in mitochondrial RNA processing (FASTKD5, DHX30) as well as in ribosomal biogenesis [50,51]. These data raise the possibility that FMRpolyG may interact and sequester the proteins which translocate to mitochondria and regulate RNA processing and translation of mitochondrial DNA encoded transcripts. This hypothesis supports our observation as it showed decreased level of mitochondrial DNA encoded transcripts in FMRpolyG expression in cells, transgenic mice and brain of FXTAS patients. Furthermore, FMRpolyG interacts with LAP2β [27], a nuclear protein important for nuclear lamina organization. Thus, it is possible that the FMRpolyG-LAP2β interaction alters transport of nuclear encoded mitochondrial transcripts to the cytosol or mitochondria. It is important to further investigate whether the dysregulated assembly of mitochondrial supercomplexes observed in FXTAS cell and animal models can originate from alterations in the nuclear export of nuclear DNA encoded transcripts and/or alterations in the RNA processing of mitochondrial DNA encoded transcripts.

In conclusion, this study provides several evidences suggesting that CGG repeats RAN translated into the FMRpolyG protein forms cytosolic small aggregates that interacts with mitochondria and potentially alters mitochondrial activities. Given the importance of mitochondrial dysfunctions in neurodegenerative diseases, including Parkinson's disease, and some overlap of symptoms between FXTAS and parkinsonism, it will be important to further study the cause and evolution of mitochondrial dysfunctions during FXTAS pathogenesis. The modulation assembly of supercomplexes by FMRpolyG as observed here, should be further explored in large cohort of FXTAS patients so that therapeutics targeting mitochondria can be evaluated.

Transparency Document

The Transparency document associated with this article can be found in the online version.

Acknowledgements

The current research work was financially supported by the Department of Science and Technology, Government of India, Indo-French grant (DST/ANR2014/Neuro-1/FXTAS) to Prof. Rajesh Singh (Indian investigator) and Dr. Nicolas Charlet Berguerand (French investigator). This work constitutes part of the Ph.D. thesis of Dhruv Gohel. Lakshmi Sripada and Kritarth Singh received Senior Research fellowships from University Grant Commission (UGC), Government of India. The MS University of Baroda sponsored by DBT Govt. of India. Authors also acknowledge the FIST program supported by DST, Govt of India.

Appendix A. Supplementary data

Supplementary data to this article can be found online at https://doi.org/10.1016/j.bbadis.2019.02.010.

References

[1] A. James, et al., Fragile X Premutation Tremor/Ataxia Syndrome: Molecular, Clinical, and Neuroimaging Correlates Se, (2003), pp. 869–878.
[2] P.J. Hagerman, R.J. Hagerman, Fragile X – Associated Tremor/Ataxia Syndrome,

vol. 1338, (2015), pp. 58–70.
[3] S. Jacquemont, et al., Penetrance of the Fragile X–Associated Tremor/Ataxia Syndrome, JAMA 291 (4) (2004) 460–469.
[4] C.T. Ashley Jr., K.D. Wilkinson, D. Reines, S.T. Warren, FMR1 protein: conserved RNP family domains and selective RNA binding, Science 262 (5133) (1993) 563–566.
[5] L.N. Smith, et al., Fragile X mental retardation protein regulates synaptic and behavioral plasticity to repeated cocaine administration, Neuron 82 (3) (2014) 645–658.
[6] R. Tabet, E. Moutin, J.A.J. Becker, D. Heintz, L. Fouillen, E. Flatter, Fragile X Mental Retardation Protein (FMRP) Controls Diacylglycerol Kinase Activity in Neurons, Proc. Natl. Acad. Sci. U. S. A. 113 (26) (2016) 3619–3628.
[7] D.L. Nelson, H.T. Orr, S. Warren, The unstable repeats-three evolving faces of neurological disease, Neuron 77 (5) (2013) 825–843.
[8] R.J. Hagerman, et al., Intention tremor, parkinsonism, and generalized brain atrophy in male carriers of fragile X, Neurology 57 (1) (2001) 127–130.
[9] J. Hunter, O. Rivero-Arias, A. Angelov, E. Kim, I. Fotheringham, J. Leal, Epidemiology of fragile X syndrome: a systematic review and meta-analysis, Am. J. Med. Genet. Part A 164 (7) (2014) 1648–1658.
[10] F. Tassone, et al., FMR1 CGG allele size and prevalence ascertained through newborn screening in the United States, Genome Med. 4 (12) (2012) 100.
[11] F. Tassone, C. Iwahashi, P.J. Hagerman, FMR1 RNA within the intranuclear inclusions of fragile X-associated tremor/ataxia syndrome (FXTAS), RNA Biol 1 (2) (2004) 103–105.
[12] R.A.M. Buijsen, et al., FMRpolyG-positive Inclusions in CNS and non-CNS Organs of a Fragile X Premutation Carrier With Fragile X-associated Tremor/Ataxia Syndrome, Acta Neuropathol. Commun. 2 (162) (2014) 1–5.
[13] F. Tassone, R.J. Hagerman, A.K. Taylor, L.W. Gane, T.E. Godfrey, P.J. Hagerman, Elevated Levels of FMR1 mRNA in Carrier Males: A New Mechanism of Involvement in the Fragile-X Syndrome, Am. J. Hum. Genet. 66 (1) (2000) 6–15.
[14] F. Tassone, et al., Elevated FMR1 mRNA in Premutation Carriers is due to Increased Transcription, RNA 13 (4) (2007) 555–562.
[15] B.A. Oostra, R. Willemsen, A Fragile Balance: FMR1 Expression Levels, Hum. Mol. Genet. 12 (2) (2003) 249–257.
[16] P. Jin, et al., RNA-Mediated Neurodegeneration Caused by the Fragile X Premutation rCGG Repeats in Drosophila, Neuron 39 (2003) 739–747.
[17] R.K. Hukema, et al., Reversibility of Neuropathology and Motor Deficits in an Inducible Mouse Model for FXTAS, Hum. Mol. Genet. 24 (17) (2015) 4948–4957.
[18] G. Hoem, et al., CGG-repeat Length Threshold for FMR1 RNA Pathogenesis in a Cellular Model for FXTAS, Hum. Mol. Genet 20 (11) (2011) 2161–2170.
[19] V. Hashem, et al., Ectopic Expression of CGG Containing mRNA is Neurotoxic in Mammals, Hum. Mol. Genet 18 (13) (2018) 2443–2451.
[20] A. Entezam, et al., Regional FMRP Deficits and Large Repeat Expansions Into the Full Mutation Range in a New Fragile X Premutation Mouse Model, Gene 395 (2007) 125–134.
[21] P.K. Todd, et al., Article CGG repeat-associated translation mediates neurodegeneration in fragile X tremor Ataxia syndrome, Neuron 78 (3) (2013) 440–455.
[22] O.A. Sofola, et al., Suppress Fragile X CGG Premutation Repeat-Induced Neurodegeneration in a Drosophila Model of FXTAS, Neuron. 55 (4) (2007) 565–571.
[23] C. Sellier, et al., Article sequestration of DROSHA and DGCR8 by expanded CGG RNA repeats alters MicroRNA processing in fragile X-associated tremor/ataxia syndrome identification of proteins associated with expanded, Cell Rep. 3 (3) (2013) 869–880.
[24] T. Kolbe, et al., Article mtDNA Segregation in Heteroplasmic Tissues is Common in vivo and Modulated by Haplotype Differences and Developmental Stage, Cell Rep 7 (6) (2014) 2031–2041.
[25] P. Jin, et al., Article Pur a Binds to rCGG Repeats and Modulates Repeat-Mediated Neurodegeneration in a Drosophila Model of Fragile X Tremor/Ataxia Syndrome, Neuron. 55 (4) (2007) 556–564.
[26] C.K. Iwahashi, et al., Protein Composition of the Intranuclear Inclusions of FXTAS, (2006), pp. 256–271.
[27] C. Sellier, et al., Translation of expanded CGG repeats into FMRpolyG Is pathogenic and may contribute to fragile X tremor ataxia syndrome, Neuron (2017) 331–347.
[28] M.G. Kearse, et al., CGG repeat-associated non-AUG translation utilizes a cap-dependent scanning mechanism of initiation to produce toxic proteins short article CGG repeat-associated non-AUG translation utilizes a cap-dependent scanning mechanism of initiation to produce toxi, Mol. Cell 62 (2) (2016) 314–322.
[29] M.I. Alvarez-Mora, L. Rodriguez-Revenga, I. Madrigal, M. Guitart-Mampel, G. Garrabou, M. Milà, Impaired Mitochondrial Function and Dynamics in the Pathogenesis of FXTAS, Mol. Neurobiol. 54 (9) (2017) 6896–6902.
[30] R.K. Hukema, et al., Induced Expression of Expanded CGG RNA Causes Mitochondrial dysfunction in vivo, Cell Cycle 13 (16) (2014) 2600–2608.
[31] C. Giulivi, E. Napoli, F. Tassone, J. Halmai, R. Hagerman, Plasma Metabolic Profile Delineates Roles for Neurodegeneration, Pro-inflammatory Damage and Mitochondrial Dysfunction in the FMR1 Premutation, Biochem. J. 473 (21) (2016) 3871–3888.
[32] S. Filipovic-Sadic, et al., A novel FMR1 PCR method for the routine detection of low abundance expanded alleles and full mutations in fragile X syndrome, Clin. Chem. 56 (3) (2010) 399–408.
[33] F. Tassone, R. Pan, K. Amiri, A.K. Taylor, P.J. Hagerman, A rapid polymerase chain reaction-based screening method for identification of all expanded alleles of the fragile X (FMR1) gene in newborn and high-risk populations, J. Mol. Diagn. 10 (1) (2008) 43–49.
[34] P. Prajapati, L. Sripada, K. Singh, K. Bhatelia, R. Singh, R. Singh, Biochimica et Biophysica Acta TNF- α regulates miRNA targeting mitochondrial complex-I and induces cell death in dopaminergic cells, Biochim. Biophys. Acta (BBA) - Mol. Basis Dis. 1852 (3) (2015) 451–461.
[35] S.M. Smith, M.B. Wunder, D.A. Norris, Y.G. Shellman, A Simple Protocol for Using a LDH-Based Cytotoxicity Assay to Assess the Effects of Death and Growth Inhibition at the Same Time, PLoS One 6 (11) (2011).
[36] P. Jha, X. Wang, J. Auwerx, Analysis of Mitochondrial Respiratory (BN-PAGE), Curr. Protoc. Mouse Biol. 6 (2016) 1–14.
[37] M.R. Green, J. Sambrook, Isolation of High-Molecular-Weight DNA Using Organic Solvents, Cold Spring Harb Protoc. (2017) 356–360.
[38] A.N. Malik, R. Shahni, A. Rodriguez-de-ledesma, A. Laftah, P. Cunningham, Biochemical and biophysical research communications mitochondrial DNA as a non-invasive biomarker: accurate quantification using real time quantitative PCR without co-amplification of pseudogenes and dilution bias, Biochem. Biophys. Res. Commun. 412 (1) (2011) 1–7.
[39] E.R. Whittemore, Peroxide-induced Cell Death in Primary Neuronal Culture, Neuroscience. 61 (4) (1995).
[40] J. Li, J. Yuan, Caspases in Apoptosis and Beyond, Oncogene (2008) 6194–6206.
[41] S. Elmore, Apoptosis: a review of programmed cell death, Toxicol. Pathol. 35 (4) (2007) 495–516.
[42] D.C. Cox, T.A. Cooper, Non-canonical RAN translation of CGG repeats has canonical requirements, Mol. Cell 62 (2) (2016) 155–156.
[43] R.C. Scaduto, L.W. Grotyohann, Measurement of mitochondrial membrane potential using fluorescent rhodamine derivatives, Biophys. J. 76 (1 Pt 1) (1999) 469–477.
[44] E. Lapuente-Brun, et al., Supercomplex assembly determines electron flux in the mitochondrial electron transport chain, Science 340 (6140) (2013) 1567–1570 (80-.).
[45] R. Acín-Pérez, P. Fernández-Silva, M.L. Peleato, A. Pérez-Martos, J.A. Enriquez, Respiratory active mitochondrial Supercomplexes, Mol. Cell 32 (4) (2008) 529–539.
[46] M.L. Genova, G. Lenaz, Functional role of mitochondrial respiratory supercomplexes, Biochim. Biophys. Acta Bioenerg. 1837 (4) (2014) 427–443.
[47] J. Montoya, M.J. López-Pérez, E. Ruiz-Pesini, Mitochondrial DNA transcription and diseases: past, present and future, Biochim. Biophys. Acta Bioenerg. 1757 (9–10) (2006) 1179–1189.
[48] C. Ross-Inta, et al., Evidence of mitochondrial dysfunction in fragile X-associated tremor/ataxia syndrome, Biochem. J. 429 (3) (2010) 545–552.
[49] D.Z. Loesch, et al., Evidence for the toxicity of bidirectional transcripts and mitochondrial dysfunction in blood associated with small CGG expansions in the FMR1 gene in patients with parkinsonism, Genet. Med. 13 (5) (2011) 392–399.
[50] O. Rackham, et al., Hierarchical RNA processing is required for mitochondrial ribosome assembly, Cell Rep. 16 (7) (2016) 1874–1890.
[51] H. Antonicka, E.A. Shoubridge, Mitochondrial RNA granules are centers for post-transcriptional RNA processing and ribosome biogenesis, Cell Rep. 10 (6) (2015) 920–932.